Modeling Phase Separation in Nonstoichiometric Silica

V. M. Burlakov,[1,*] G. A. D. Briggs,[1] A. P. Sutton,[1,†] Angelo Bongiorno,[2] and Alfredo Pasquarello[2]

[1]*Department of Materials, University of Oxford, Parks Road, Oxford OXI 3PH, United Kingdom*
[2]*Institute de Théorie des Phénoménes Physiques (ITP), Ecole Polytechnique Fédérale de Lausanne (EPDL), CH-1015 Switzerland
and Institut de Recherche Numérique en Physique des Matériaux (IRRMA), CH-1015 Lausanne, Switzerland*

We have modeled the decomposition of nonstoichiometric amorphous SiO$_x$ upon annealing into silicon and stoichiometric silica, using a new method based on mapping Metropolis Monte Carlo simulations onto rate equations. The concentrations of all oxidation states of silicon are derived as a function of time and found to attain steady-state values at long times dependent on temperature T and oxygen content x. The degree of phase separation and the sizes of Si particles are predicted as a function of T and x, enabling greater control over the size of silicon quantum dots in silica matrices.

           PACS numbers: 61.43.Bn, 68.35.–p

Nonstoichiometric amorphous silica (SiO$_x$) has attracted interest in a wide range of fields within physical science (see, for example, [1–6]). It is also widely used in industry for protective layers, optical coatings, insulating layers, and gas-barrier layers [7–11]. Some experimental studies [1] suggest the bulk SiO$_x$ with $x \sim 1$ consists of a mixture of pure SiO$_2$ and Si phases, separated by layers comprising Si atoms in intermediate oxidation states. Other experiments [2–4] in which amorphous SiO$_2$/SiO/SiO$_2$ superlattices were annealed yielded a homogeneous array of Si quantum dots within the Si-O layers, the size of the dots depending on the layer thickness and annealing conditions. These results suggest that SiO$_x$ tends to separate into pure Si and SiO$_2$. In this Letter, we present a new and remarkably simple method to model the decomposition of SiO$_x$ into pure Si and SiO$_2$ as a function of time, temperature, and composition. We find that the degree of phase separation reaches a constant value at long annealing times, and we predict steady-state sizes of Si particles in SiO$_2$ matrices and of SiO$_2$ particles in Si matrices as a function of T and x (Fig. 3).

Assuming that (a) each oxygen atom is always bonded to two silicon atoms, and (b) each silicon atom has four nearest neighbors, then the numbers of Si-O and Si-Si bonds in SiO$_x$ are conserved throughout separation. Therefore, there must be an additional contribution to the energy of the system beyond a sum of Si-O and Si-Si bond energies to drive separation. The origin of this additional term is nonpairwise and it is known as the suboxide penalty energy (a Si atom with 1, 2, or 3 oxygen neighbors is called a silicon suboxide). Suboxide penalty energies were obtained *ab initio* either from periodic suboxide models [12] or from suitable Si-O clusters [13].

The Metropolis Monte Carlo (MC) technique with moves involving the exchange of pairs of nearest neighbors of bonded Si atoms [14] is widely used for simulating amorphous Si and SiO$_2$ structures and interfaces between them [15]. In this Letter, we apply this approach to nonstoichiometric silica. To obtain an acceptance ratio of at

least 1% we find that the simulation temperature has to be very high, and at some compositions it is almost certainly above the real melting point. The simulation of phase separation is very slow even at such high temperatures. We present a new approach to model the phase separation by mapping the Metropolis Monte Carlo procedure onto rate equations for average concentrations of all possible oxidation states (OS) of Si in SiO$_2$. Our approach enables us to model phase separation at realistic temperatures over much longer times than can be achieved in Monte Carlo simulations for the same CPU time.

Phase separation in nonstoichiometric silica is effected by diffusion of oxygen. Consider a Si atom with $1 \leq k \leq 3$ oxygen nearest neighbors, so that of its four nearest neighbors, at least one is an oxygen atom and at least one is a silicon atom. The value of k is defined as the OS of the Si atom, and Si atoms with k oxygen neighbors are denoted by Si(k). Consider a bond between a Si(k) atom and one of its k neighboring oxygen atoms. Let the OS of the other Si atom to which the oxygen is bonded be i, where $1 \leq i \leq 4$. Let one of the Si-Si bonds to the same Si(k) atom be to a Si(j) atom, where $0 \leq j \leq 3$. The fundamental diffusional step involves translation of the oxygen atom from the bond between Si(k) and Si(i) and insertion into the adjacent bond between Si(k) and Si(j). After such a step k does not change, but $i \rightarrow i - 1$ and $j \rightarrow j + 1$. Assuming a *random* distribution of all OS, the probabilities of choosing a neighboring pair, Si(k), and Si(l), which have (P_{kl}^{ox}) or have not (P_{kl}^{nox}) a common oxygen atom between them are

$$P_{kl}^{ox}(t) = \frac{kl}{4} \frac{n_k(t)n_l(t)}{Z^{ox}(t)},$$

$$P_{kl}^{nox}(t) = \frac{(4-k)(4-l)}{4} \frac{n_k(t)n_l(t)}{Z^{max}(t)}, \tag{1}$$

where $n_k(t)$ and $n_l(t)$ are the concentrations of Si(k) and Si(l) atoms at time t. Since the overall probability of finding Si(k) is $\sum_l [P_{kl}^{ox}(t) + P_{kl}^{nox}(t)] = n_k(t)$, the normal-

ization factors are given by

$$Z^{ox}(t) = \sum_l l n_l(t), \qquad Z^{nox}(t) = \sum_l (4-l) n_l(t). \quad (2)$$

The probability $\tilde{P}_{ij}$ that an oxygen atom bonded to a Si(i) atom neighbors a Si-Si bond to a Si(j) atom can then be defined as

$$\tilde{P}_{ij}(t) = \frac{n_i(t) n_j(t) i (4-j)}{12 Z_{ox}(t) Z_{nox}(t)} \sum_k n_k(t) k (4-k). \quad (3)$$

We follow Metropolis MC and assume that the probability of an oxygen jump depends on the energy difference between the initial and the final states of the system. Oxygen diffusion is much slower than the associated relaxation processes; therefore, we assume that the system is always elastically relaxed. The probability of an oxygen jump is governed only by the suboxide penalty energies Δ_i in the initial and final states. The energies Δ_i for Si(i) are from Ref. [13]: $\Delta_1 = 0.5$ eV, $\Delta_2 = 0.51$ eV, $\Delta_3 = 0.22$ eV, and $\Delta_0 = \Delta_4 = 0$. The probability $W_{i,j}(t)$ that at time t an oxygen atom bonded to a Si(i) atom jumps into a neighboring Si-Si bond to a Si(j) atom is thus

$$W_{i,j}(t) = \frac{\tilde{P}_{ij}(t)}{Z} \min\left\{1, \exp\left(-\frac{E_{final} - E_{init}}{kT}\right)\right\}, \quad (4)$$

where Z is a normalization constant with which we determine the time scale, k is the Boltzmann constant, and T is the system temperature. The factor min $\{1, \exp[-(E_{final} - E_{init})/kT]\}$ in Eq. (4) is equal to unity if the energy of the final state $E_{final} = \Delta_{i-1} + \Delta_{j+1}$ is lower than that of the initial state $E_{init} = \Delta_i + \Delta_j$, otherwise it is equal to the Boltzmann factor.

The evolution of the concentration of oxidation state $n_i(t)$ is determined by a set of coupled nonlinear rate equations:

$$\frac{dn_i(t)}{dt} = \sum_{j=0}^{3} W_{i,j}(t) + \sum_{j=0}^{3} W_{i+1,j}(t) + \sum_{j=1}^{4} W_{j,i-1}(t)$$
$$- \sum_{j=1}^{4} W_{j,i}(t). \quad (5)$$

Equations (1)–(5) are solved numerically using some initial concentrations of the oxidation states at temperature T. To validate our rate-equation (RE) model, we compared its solutions with results obtained from MC simulations for the same annealing temperature. First we generated a number of amorphous SiO$_x$ structures by simulated deposition using our recently developed method [16]. At this stage, the suboxide penalty energies were set to zero. The structures were then annealed for about 10^6 MC steps taking into account suboxide penalty energies. The annealing temperature was optimized for each particular structure to have a reasonable acceptance rate of MC moves. During annealing, moves included

both the motion of dangling bonds [16] and the switching of pairs of bonds [14], the combination enabling more complete relaxation of the elastic energy.

Using the initial OS concentrations obtained immediately after deposition of amorphous SiO$_x$, we calculated their evolution during annealing using our RE approach for comparison with our MC simulations. Figure 1 compares the results obtained by both methods for SiO$_{1.7}$ and SiO$_{0.33}$. It is seen that the RE model reproduces the results of the MC simulations well. In addition, we found that for a given composition, the final concentrations of OS obtained within the RE model do not depend on their initial values, indicating that a true steady state is reached. This steady-state solution describes an equilibrium configuration of the system. It is not the ground-state configuration of the system, which would display some degree of crystallization. Such a configuration is inaccessible in our model because we neglect the strain energy.

Our rate-equation approach is more than a million times faster than the Metropolis Monte Carlo simulations. As seen in Fig. 1, we are able to extend the simulation time of the phase separation process by several orders of magnitude using the rate equations.

Figure 2 shows the x dependence of the steady-state OS concentrations in annealed SiO$_x$. We see that at all x, the
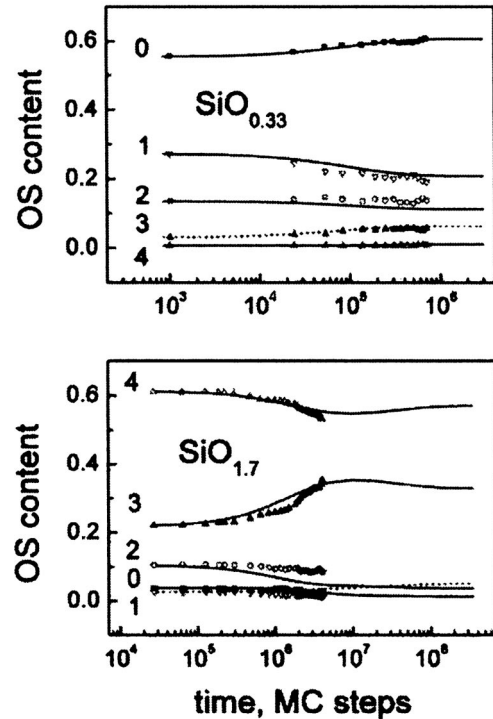

FIG. 1. Time evolution of OS concentrations in amorphous SiO$_{0.33}$ and SiO$_{1.7}$. Symbols: MC results for $kT = 0.35$ eV(SiO$_{0.33}$) and $kT = 0.15$ eV(SiO$_{1.7}$). Curves: RE results for the same temperatures. The time scale in the RE model is adjusted through the parameter Z in Eq. (4) to give best fit to MC results. Curves are labeled according to OS.
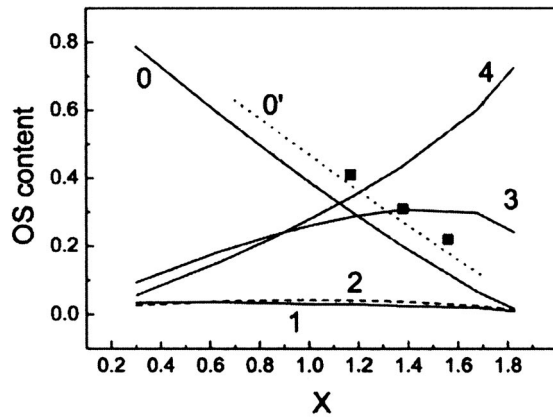
FIG. 2. Steady-state OS concentrations as a function of x. Curves labeled 0, 1, 2, 3, and 4 correspond to Si(i), and were obtained within the RE model [using Eqs. (6) and (7)] at $T = 1250\,°C$. Symbols represent experimental data for the content of Si(0) in the bulk SiO_x annealed at $T = 1250\,°C$ [18]. The curve 0′ shows RE results for Si(0) at $T \approx 600\,°C$.

system comprises primarily Si(0), Si(4), and suboxide Si(3), indicating phase separation into Si and SiO_2 with interfaces containing Si(3). The dominance of Si(3) at these interfaces is consistent with experimental observations reported in [17]. We found that the concentrations of Si(1) and Si(2) start to rise only at temperatures above ~1200 °C. In Fig. 2, we also show experimental values for Si(0) content obtained after annealing SiO_x at $T = 1250\,°C$ for about 1 h [18]. The experimental values are slightly higher than those calculated for $T = 1250\,°C$ within the RE model.

We may estimate the size of pure Si clusters by calculating an average surface-to-volume ratio for the clusters, corresponding to the ratio of the number of Si atoms with fewer than four Si(0) neighbors to the number of Si(0) atoms within the clusters. Since we have assumed a random distribution of OS, the probability P_S for a Si atom to be on the cluster surface, i.e., to have $k = 1$ or 2 neighboring suboxides Si(i) ($i = 1, 2, 3$), and the probability P_V for a Si atom to be anywhere in the cluster are

$$P_S \simeq \sum_{k=1}^{2} \frac{4!}{k!(4-k)!} P_0^k P_1^{4-k}, \qquad P_V = P_S + P_0^4, \quad (6)$$

where $P_0 = 4n_0$, $P_1 = \sum_{i=1}^{3}(4-i)n_i$, and n_i is the steady-state concentration of the ith OS. To avoid overestimation of Si clusters surface area, we do not count Si(0) atoms having three neighboring suboxides as belonging to Si clusters. As we will be interested in the ratio of P_S/P_V, the probabilities P_S and P_V do not have to be normalized. Assuming that all clusters are identical spheres of diameter D_{cl}, we obtain $D_{cl} = 2R$ from the equation

$$P_S/P_V = [R^3 - (R - d)^3]/R^3. \quad (7)$$

The value of the thickness d of a monatomic layer on the cluster surface can be estimated as $d = \rho^{-1/3} \simeq 0.27$ nm, where the density of amorphous Si is taken to be $\rho \simeq 0.05$ atoms$/^3$. Substituting the steady-state concentrations of OS at $T = 1250\,°C$ into Eqs. (6) and (7), we obtain the diameter of Si clusters as a function of x, shown by the broken line in Fig. 3. The symbols in Fig. 3 show experimentally determined average diameters of Si nanocrystals at $T = 1250\,°C$ and 1100 °C.

It is seen in Fig. 3 that the experimental values of nanocrystal sizes are about 2 times higher than those estimated using Eqs. (6) and (7) for a temperature $T = 1250\,°C$. This discrepancy indicates that our assumption of a random distribution of OS [implicit in the use of $W_{i,j}(t)$ as a parameter independent of cluster size] breaks down. One possible reason is Ostwald ripening [19], which would decrease the surface-to volume ratio, as compared with the prediction of Eq. (6). However, we note that the experimental observations of steady-state cluster sizes after sufficiently long anneals indicate that the ripening process is eventually suppressed, presumably by the development of elastic accommodation stresses, which are directly proportional to the cluster volume [20].

Despite the breakdown of our assumption of a random distribution of OS, we find that the increase in the average cluster size can still be described by the RE model by reducing the temperature at which phase separation is assumed to occur. This is seen in Fig. 3 where the solid line shows the prediction for an assumed growth temperature of ~600 °C. A similar improvement between the prediction of the RE model and experiment for the overall content of Si phase is obtained also with a growth temperature of ~600 °C (curve 0′ in Fig. 2). These observations indicate that the influence of nonrandomness
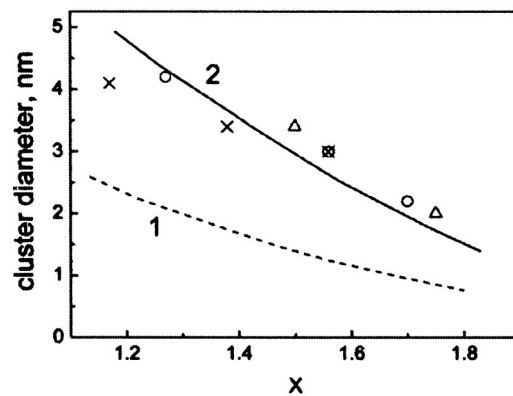

FIG. 3. Lines: average Si cluster diameter as a function of x at (1) $T = 1250\,°C$ and (2) ~600 °C, as calculated using Eqs. (6) and (7). Symbols are experimental values of the average size of Si nanocrystals: circles [21] and crosses [18] are for bulk SiO_x annealed at $T = 1250\,°C$, triangles are for $SiO_2/SiO/SiO_2$ superlattice annealed at $T = 1100\,°C$ [3].

of the distributions of OS in real systems may be reproduced in the RE model by assuming a lower temperature of phase separation, or, according to Eq. (4), correspondingly higher suboxide penalty energies.

In conclusion, we have derived a set of rate equations based on the Metropolis Monte Carlo procedure, and shown that SiO_x tends to separate into Si and SiO_2 clusters at all temperatures of experimental relevance. Our rate equations enabled phase separation throughout more of the temperature-oxygen content space to be explored than can be modeled with Monte Carlo simulations. The solution of the rate-equation yielded steady-state concentrations of various OS of Si, the degree of phase separation, and the expected sizes of Si particles. This work provides a means of predicting the sizes of Si quantum dots embedded in SiO_2, formed by annealing SiO_x at various values of x and temperature, as seen experimentally in Refs. [2–4]. Similar analysis can be performed also for SiO_2 particles in Si matrix.

———————

*On leave from the Institute for Spectroscopy, Russian Academy of Sciences, Troitsk, Moscow region, 142090, Russia

[†]Also Helsinki University of Technology, Laboratory of Computational Engineering, PO Box 9203, FIN-02015 HUT, Finland.

[1] T. Hohl, P. A. Wieder, T. E. van Aken, G. Weirich, M. Denninger, S. Vidal, C. Oswald, J. Deneke, H. Mayer, and J. Fuess, J. Non-Cryst. Solids **320**, 255 (2003).

[2] M. Zacharias, J. Heitmann, and U. Goesele, MRS Bulletin Vol. 26 No. 12, edited by Luis M. Liz-Marzan and David Norris (p. 975, Dec. 2000).

[3] M. Zacharias, J. Heitmann, R. Scholz, U. Kahler, M. Schmidt, and J. Biasing, Appl. Phys. Lett. **80**, 661 (2002).

[4] L. X. Yi, J. Heitmann, R. Scholz, and M. Zacharias, Appl. Phys. Lett. **81**, 4248 (2002).

[5] K. Sato, T. Izumi, M. Iwase, Y. Show, H. Morisaki, T. Yaguchi, and T. Kamino, Appl. Surf. Sci. **216**, 376 (2003).

[6] S. Wada, Y. Murata, A. T. Tokunaga, and J. Watanabe, Astron. Astrophys. **406**, 783 (2003).

[7] G. Hassand and C. D. Salzberg, J. Opt. Soc. Am. **44**, 181 (1954).

[8] M. J. O'Leary and J. H. Thomas III, J. Vac. Sci. Technol. A **5**, 106 (1987).

[9] J. U. Schmidt and B. Schmidt, Mater. Sci. Eng., B **101**, 28 (2003).

[10] C. A. Wang, R. K. Huang, D. A. Shiau, M. K. Connors, P. G. Murphy, P. W. O'Brien, A. C. Anderson, D. M. DePoy, G. Nichols, and M. N. Palmisiano, Appl. Phys. Lett. **83**, 1286 (2003).

[11] M. S. Hedenqvist and K. S. Johansson, Surf. Coat. Technol. **172**, 7 (2003).

[12] D. R. Hamann, Phys. Rev. B **61**, 9899 (2000).

[13] A. Bongiorno and A. Pasquarello, Phys. Rev. B **62**, R16326 (2000).

[14] F. Wooten, K. Winer, and D. Weaire, Phys. Rev. Lett. **54**, 1392 (1985).

[15] Y. Tu and J. Tersoff, Phys. Rev. Lett. **84**, 4393 (2000).

[16] V. M. Burlakov, G. A. D. Briggs, A. P. Sutton, and Y. Tsukahara, Phys. Rev. Lett. **86**, 3052 (2001).

[17] F. Rochet, Ch. Poncey, G. Dufour, H. Roulet, C. Guillot, and F. Sirotti, J. Non-Cryst. Solids **216**, 148 (1997); A. Barranco, F. Yubero, J. P. Espinos, J. P. Caballero, A. R. Gonzalez-Elipe, and J. A. Mejias, Vacuum **67**, 491 (2002).

[18] L. Dal Negro, M. Cazzanelli, N. Daldosso, Z. Gaburro, L. Pavesi, F. Priolo, D. Pacifici, G. Franzò, and F. Iacona, Physica E (Amsterdam) **16**, 297 (2003).

[19] A. P. Sutton and R. W. Balluffi, *Interfaces in Crystalline Materials* (Oxford University Press, New York, 1995), p. 628-633.

[20] J. D. Eshelby, Proc. R. Soc. London A **241**, 376 (1957).

[21] F. Iacona, G. Franzò, and C. Spinella, J. Appl. Phys. **87**, 1295 (2000).